REPORT DOCUMENTATION PAGE

Form Approved OMB NO. 0704-0188

1. REPORT DATE (DD-MM-YYYY)	2. REPORT TYPE	3. DATES COVERED (From - To)
	New Reprint	-

4. TITLE AND SUBTITLE	5a. CONTRACT NUMBER
Contactless Microwave Measurements of Photoconductivity in Silicon Hyperdoped with Chalcogens	W911NF-09-1-0470
	5b. GRANT NUMBER
	5c. PROGRAM ELEMENT NUMBER
	622624

6. AUTHORS	5d. PROJECT NUMBER
David Hutchinson, Thomas Cruson, Anthony DiFranzo, Andrew McAllister, Aurore J. Said, Jeffrey M. Warrender, Daniel Recht, Peter D. Persans, Michael J. Aziz	
	5e. TASK NUMBER
	5f. WORK UNIT NUMBER

7. PERFORMING ORGANIZATION NAMES AND ADDRESSES	8. PERFORMING ORGANIZATION REPORT NUMBER
Rensselaer Polytechnic Institute Office of Sponsored Research Rensselaer Polytechnic Institute Troy, NY 12180 -	

9. SPONSORING/MONITORING AGENCY NAME(S) AND ADDRESS(ES)	10. SPONSOR/MONITOR'S ACRONYM(S)
U.S. Army Research Office P.O. Box 12211 Research Triangle Park, NC 27709-2211	ARO
	11. SPONSOR/MONITOR'S REPORT NUMBER(S)
	57225-EL.5

12. DISTRIBUTION AVAILIBILITY STATEMENT
Approved for public release; distribution is unlimited.

13. SUPPLEMENTARY NOTES
The views, opinions and/or findings contained in this report are those of the author(s) and should not contrued as an official Department of the Army position, policy or decision, unless so designated by other documentation.

14. ABSTRACT

Photoconductivity in silicon hyperdoped with sulfur and selenium above the insulator-to-metal transition was measured via photoinduced changes in the microwave reflectivity of hyperdoped layers formed on p-type silicon. Despite these materials' strong subgap optical absorption, exposing them to 1310 and 1550nm light results in a change in conductivity per photon 10,000 times smaller than what is observed in untreated silicon exposed to 980nm light. A similar bound applies for 405nm light, which is absorbed entirely in the hyperdoped layer. We use

15. SUBJECT TERMS
photoconductivity, photocarrier lifetime, hyperdoped silicon

16. SECURITY CLASSIFICATION OF:			17. LIMITATION OF ABSTRACT	15. NUMBER OF PAGES	19a. NAME OF RESPONSIBLE PERSON
a. REPORT	b. ABSTRACT	c. THIS PAGE			Peter Persans
UU	UU	UU	UU		19b. TELEPHONE NUMBER
					518-276-2934

Standard Form 298 (Rev 8/98)
Prescribed by ANSI Std. Z39.18

Report Title

Contactless Microwave Measurements of Photoconductivity in Silicon Hyperdoped with Chalcogens

ABSTRACT

Photoconductivity in silicon hyperdoped with sulfur and selenium above the insulator-to-metal transition was measured via photoinduced changes in the microwave reflectivity of hyperdoped layers formed on p-type silicon. Despite these materials' strong subgap optical absorption, exposing them to 1310 and 1550nm light results in a change in conductivity per photon 10,000 times smaller than what is observed in untreated silicon exposed to 980nm light. A similar bound applies for 405nm light, which is absorbed entirely in the hyperdoped layer. We use these results to deduce that the photocarrier lifetime in the hyperdoped material is □100 ns.

REPORT DOCUMENTATION PAGE (SF298)
(Continuation Sheet)

Continuation for Block 13

ARO Report Number   57225.5-EL
Contactless Microwave Measurements of Photo   ...

Block 13: Supplementary Note

Contactless Microwave Measurements of Photoconductivity in Silicon Hyperdoped with Chalcogens

Daniel Recht, David Hutchinson[1], Thomas Cruson[1], Anthony DiFranzo[1], Andrew McAllister[1], Aurore J. Said, Jeffrey M. Warrender[2], Peter D. Persans[1], and Michael J. Aziz*

Harvard School of Engineering and Applied Sciences, Cambridge, MA 02138, U.S.A.
[1]Department of Physics and Astronomy, Rensselaer Polytechnic Institute, Troy, NY 12180, U.S.A.
[2]ARDEC, Benét Laboratories, Watervliet Arsenal, NY 12189, U.S.A.

Photoconductivity in silicon hyperdoped with sulfur and selenium above the insulator-to-metal transition was measured via photoinduced changes in the microwave reflectivity of hyperdoped layers formed on p-type silicon. Despite these materials' strong subgap optical absorption, exposing them to 1310 and 1550 nm light results in a change in conductivity per photon 10,000 times smaller than what is observed in untreated silicon exposed to 980 nm light. A similar bound applies for 405 nm light, which is absorbed entirely in the hyperdoped layer. We use these results to deduce that the photocarrier lifetime in the hyperdoped material is ≤100 ns. © 2012 The Japan Society of Applied Physics

S ilicon doped to nearly 1 at. %, i.e., hyperdoped, with sulfur, selenium, or tellurium is of interest because of its sub-bandgap optical absorption and potential use in photodetectors and photovoltaics.[1–6] However, whether these materials, which have absorption coefficients, $\alpha > 10,000 \, \text{cm}^{-1}$ between silicon's band-gap and 0.2 eV, generate an electrical signal when they absorb subgap light remains unknown.[2,6] Furthermore, these materials undergo an insulator-to-metal transition and have unexplained features in their band structure, which may be due to the delocalization of impurity states.[7,8] The attribution of observations[9] of longer-than-expected carrier lifetimes in silicon hyperdoped with titanium to such delocalization has been challenged,[10] increasing the need for accurate measurements of carrier lifetime in hyperdoped silicon.

Photoinduced changes in microwave reflectivity are routinely used to measure photoconductivity without the confounding effects of electrical contacts.[11–15] In this technique, photocarriers generated by an optical pump beam lead to a small increase in the absorption of a microwave probe beam, which is detected as a decrease in the intensity of reflected microwaves. We report microwave reflectivity measurements of steady-state photoconductivity in silicon hyperdoped with S and Se by ion implantation followed by nanosecond pulsed laser melting. From these, we deduce upper bounds on the subgap photoconductivity and photocarrier lifetime in these materials.

~350 nm films doped with ^{32}S and ^{78}Se to peak concentrations approximately $(2–3) \times 10^{20}/\text{cm}^3$ were prepared using the substrates (double-side polished, 750 μm thick, 10–30 Ω cm) and the procedure described by Said *et al.*, omitting furnace annealing and contact deposition.[3] Aside from a shallower Se implant depth, the samples should be similar in properties to those characterized previously.[1] Three identically prepared samples for each dopant were measured in a microwave reflectance setup similar to that of Borrego *et al.*[15] Figure 1 shows a schematic of the microwave setup. 38 GHz microwaves emitted by a Millitech Gunn diode pass, via a waveguide, through an isolator to protect the source from reflections. A "magic tee" then splits the microwaves into two beams. One beam passes through an attenuator and is reflected back by a metallic shunt. The other
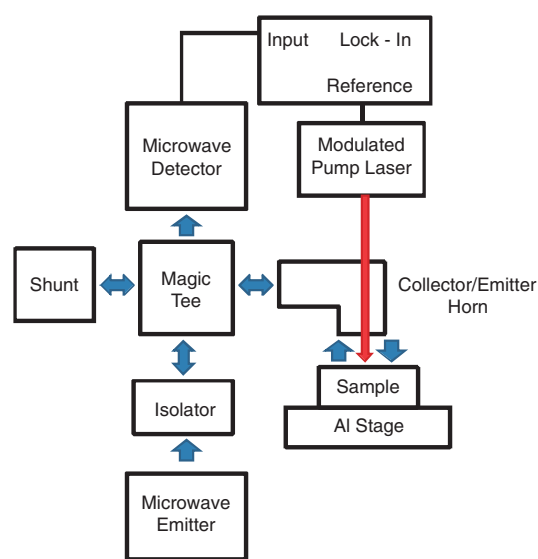
Fig. 1. Schematic diagram of microwave photoconductivity measurement apparatus.

beam emerges from a microwave emitter/collector horn and is reflected, in air, off the sample, which is mounted on an aluminum stage. The microwaves reflected from the sample and shunt then return to the magic tee where they recombine and then pass, via the tee's fourth branch, through another attenuator and into a Hewlett Packard R422A crystal detector. Path lengths for the split beams were adjusted for each sample to maximize the amount of constructive interference, and thus, the signal, at the crystal detector. A 1-mm-diameter hole was drilled in the microwave horn to allow the pump laser to illuminate the sample. Lasers were modulated at 286 Hz using a Thorlabs LDC500 laser diode controller. The photoinduced change in the intensity of reflected microwaves was recorded using a Stanford Research Systems SR530 lock-in amplifier. Laser wavelengths of 405, 650, 980, 1060, 1310, and 1550 nm were used. The signal varied linearly with laser power at all wavelengths. The power of light incident on the sample was generally kept below 3 mW to minimize heating. A higher incident power (36 mW) was used at 405 nm in an attempt to observe transient photoconductivity in the hyperdoped material using an oscilloscope. 405 nm was chosen because these materials' $\alpha > 100,000$ at this wavelength[2] provides absorption entirely

*E-mail address: maziz@harvard.edu

within the 350 nm treated layer. Many measurements of each sample were made under each set of conditions and subsequently averaged. This experiment is similar to that of Sinton and Cuevas, but with microwaves as the probe.[16]

Because the measurement involves microwave interference, we controlled for variations in sample thickness. Each sample was measured with its untreated surface resting on the stage ("down") and then measured again with its hyperdoped surface down. Because 405, 650, and 980 nm light cannot penetrate 750 μm of silicon to reach the hyperdoped layer, each sample thus provided its own untreated control at these wavelengths. Because 15% of 1060 nm light penetrates 750 μm of silicon, an additional sample was prepared where 2.7 μm (including the hyperdoped layer) were etched off using tetramethylammonium hydroxide. The signal from both sides of this sample under 1060 nm illumination was indistinguishable from a measurement of the untreated side of a hyperdoped sample.

The measured photoinduced decrease in reflected microwave intensity results from an increase in microwave absorption. This can be expressed as

$$ \text{signal} \propto \Delta A \propto \int_{\text{Sample}} \Delta \alpha_{\mu\text{wave}}(z) E^2(z)\, dz, \qquad (1) $$

where ΔA is the change in microwave absorption, $\Delta \alpha_{\mu\text{wave}}(z)$ is the change in the microwave absorption coefficient, $E(z)$ is the microwave electric field, and z is the depth. Steady-state conditions and uniform microwave illumination imply no dependence on time or the other two spatial dimensions. Because silicon is nearly transparent to microwaves while the aluminum stage is a mirror, $E(z)$ is a standing wave with a node at the stage. Silicon's microwave refractive index of 3.4 gives 38 GHz microwaves a wavelength of 2.3 mm.[17] This implies that $E(z)^2$ remains greater than 80% of its maximum in the top 350 μm of the sample and then decays smoothly with depth to the node at the stage. 405, 650, and 980 nm illuminations are thus absorbed in the region where $E(z)^2$ is nearly constant. For 1310 and 1550 nm pump wavelengths, absorbed only in the thin hyperdoped layer, $E(z)$ can be taken as constant for measurements with the hyperdoped layer up and zero with the hyperdoped layer down (at the node). Incomplete absorption in the substrate precludes the quantitative analysis of the response to the 1060 nm pump. Nevertheless, comparison with the etched sample would detect anomalous photoconductivity at 1060 nm, as might be expected from Said *et al.*[3] Although the hyperdoped layer's resistivity of roughly $0.005\,(\Omega\,\text{cm})^{-1}$ is several orders smaller than that of the substrate, the layer's thinness ensures that it will have a small effect on samples' microwave reflection and absorption in the dark.[13]

Noting that the change in absorption coefficient is proportional to the change in conductivity,[15] combining with eq. (1), and pulling $E(z)$ out of the integral yields

$$ \text{signal} \propto \int_{\text{Sample}} \Delta \sigma(z)\, dz = \int_{\text{Sample}} \Delta n(z)\mu(z)\tau(z)\, dz, \quad (2) $$

in which $\Delta \sigma(z)$ is the change in conductivity, $\Delta n(z)$ is the photocarrier concentration, $\mu(z)$ is the carrier mobility (a single mobility is sufficient for order-of-magnitude estimates), and $\tau(z)$ is the photocarrier lifetime. Under steady-state conditions, this implies that
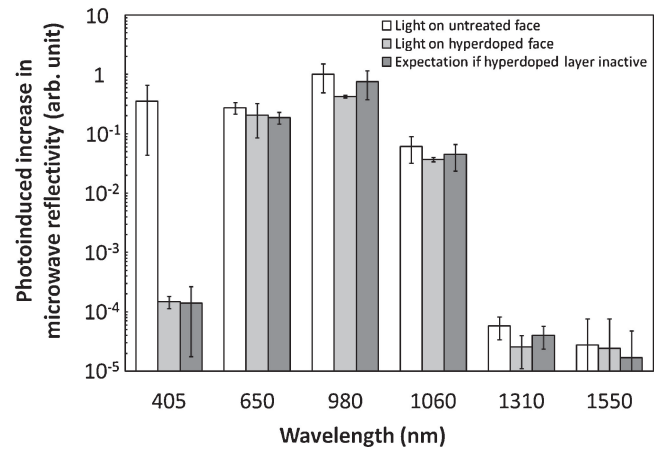
Fig. 2. Plot of the photoinduced change in microwave reflectivity as a function of pump wavelength for silicon hyperdoped with sulfur. The white bars are control data collected with the untreated side of the sample illuminated, the light gray bars are data collected with the hyperdoped side illuminated, and the dark gray bars are an estimate of the expected signal from the substrate alone when the hyperdoped side is illuminated.

$$ \text{signal} = C\Delta N\mu\tau, \qquad (3) $$

in which C is the constant of proportionality, ΔN is the total number of photocarriers generated per second, and μ and τ are averages over z weighted by the steady-state photocarrier distribution. Normalizing by the number of incident photons arriving per second gives

$$ \frac{\text{signal}}{\text{photons per second}} = C'\eta\mu\tau, \qquad (4) $$

where the constant of proportionality C' is the same for all samples (because they have identical dimensions) and all wavelengths, and η is the quantum efficiency of photocarrier generation, a material property averaged over z weighted by the steady state photon distribution. Equation (4) means that the ratio of two measurements, corrected for different photon fluxes, is the ratio of the $\eta\mu\tau$ products implied by those measurements.

Figures 2 and 3 show the average photoinduced change in microwave reflectivity for the samples of silicon hyperdoped with S and Se, respectively. The data in both plots have been normalized by the number of pump photons incident per second, accounting for reflection, and scaled so that the signal from 980 nm illumination of the untreated side is unity. Three sets of data are shown: the signal with the untreated side illuminated, the signal with the hyperdoped side illuminated, and a calculation of the signal expected from the substrate when illuminating the hyperdoped side. Error bars represent one standard deviation in the combined three-sample datasets. The calculated data are the results when illuminating the untreated side scaled by the fraction of light transmitted by the hyperdoped layer. Recombination at the untreated surface may thus cause the calculated value to underestimate the expected signal. The transmitted fraction was computed from the optical absorption and secondary ion mass spectroscopy data (used to estimate the hyperdoped layer thickness of 350 nm) in refs. 1 and 2. Data for 1060 nm illumination is included for completeness despite the difficulties in interpretation discussed above.
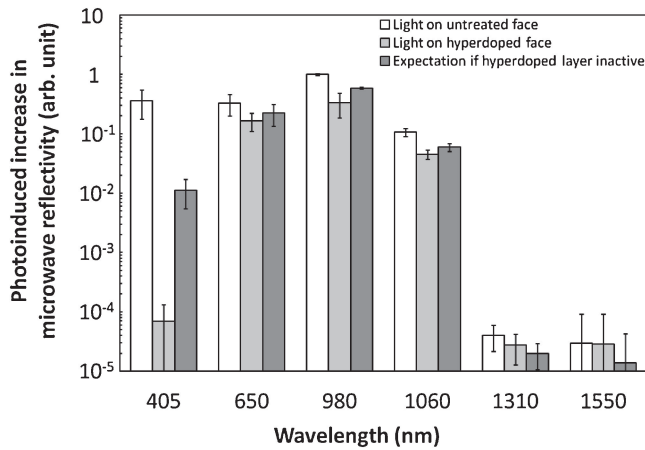
Fig. 3. Plot of the photoinduced change in microwave reflectivity as a function of pump wavelength for silicon hyperdoped with selenium. The format is identical to Fig. 2.

At all wavelengths, our measurements were unable to detect photoconductivity in the hyperdoped material. The time-dependent photoconductivity measurements at 405 nm indicated a substrate lifetime of ∼10 µs, but produced a null result for the hyperdoped material. Even though 650 nm illumination is absorbed near the n+p junction, we observed no enhanced photoconductivity at that wavelength due to charge separation. Despite the intriguing device performance at 1060 nm reported in ref. 3, we saw no evidence of anomalous photoconductivity at this wavelength either. Given that the hyperdoped layer should absorb roughly half of the unreflected light at 1550 and 1310 nm, we conclude that the photoinduced change in conductivity in hyperdoped silicon exposed to these wavelengths is at least 10,000 times smaller (on a per-photon basis) than the change in conductivity in ordinary silicon exposed to 980 nm light.[1,2] A similar statement is true for 405 nm light, which is absorbed entirely in the hyperdoped layer.

Combining this result with literature data gives an order-of-magnitude upper bound on the $\mu\tau\eta$ product of silicon hyperdoped with S and Se. The conclusion of the previous paragraph implies that

$$10^{-4} \geq \frac{f\eta_{\mathrm{h}}\mu_{\mathrm{h}}\tau_{\mathrm{h}} + (1-f)\eta_{\mathrm{Si}}\mu_{\mathrm{Si}}\tau_{\mathrm{Si}}}{\eta_{\mathrm{Si}}\mu_{\mathrm{Si}}\tau_{\mathrm{Si}}} \geq \frac{\eta_{\mathrm{h}}\mu_{\mathrm{h}}\tau_{\mathrm{h}}}{\eta_{\mathrm{Si}}\mu_{\mathrm{Si}}\tau_{\mathrm{Si}}}, \quad (5)$$

in which the subscripts h and Si represent the hyperdoped material and ordinary silicon, respectively, and f is the fraction of the signal when the hyperdoped layer is up due to carriers in the hyperdoped layer. $f < 1$ because of optical absorption below the hyperdoped layer. The second inequality holds because $\eta_{\mathrm{Si}}\mu_{\mathrm{Si}}\tau_{\mathrm{Si}} > \eta_{\mathrm{h}}\mu_{\mathrm{h}}\tau_{\mathrm{h}}$. Including carrier escape into the substrate, e.g., because of drift in an electric field caused by chalcogen concentration gradients in the hyperdoped layer,[1] would add additional terms to the first inequality in eq. (5) without changing the second. Inserting order-of-magnitude estimates for silicon's properties gives

$$10^{-4} \times 1 \times 1000 \, \mathrm{cm^2 \, V^{-1} \, s^{-1}} \times 10 \, \mu s$$
$$= 10^{-6} \, \mathrm{cm^2 \, V^{-1}} \geq \eta_{\mathrm{h}}\mu_{\mathrm{h}}\tau_{\mathrm{h}}. \quad (6)$$

References 7 and 18 indicate that $50 \, \mathrm{cm^2 \, V^{-1} \, s^{-1}}$ is a reasonable estimate for the carrier mobility in the hyper-

doped layer.[7,18] Using this in eq. (6) implies that $20 \, \mathrm{ns} \geq \eta_{\mathrm{h}}\tau_{\mathrm{h}}$. That this bound is valid for 405 nm illumination, which should cause substantial band-to-band absorption even in the hyperdoped layer (i.e., $\eta_{\mathrm{h}} > 0.2$), suggests that a short photocarrier lifetime ($\leq 100 \, \mathrm{ns}$) in the hyperdoped layer is responsible for photoconductivity being undetectable there. This is consistent with the lifetime reduction due to Auger recombination observed in silicon doped to similar concentrations with traditional dopants and/or Shockley–Read–Hall recombination in silicon with a similar number of deep traps[19] and prevents the use of this measurement to estimate the quantum efficiency of photocarrier generation associated with subgap absorption. Even though the samples measured here contain sufficient sulfur and selenium to be metallic,[6,8] our data show carrier lifetimes much smaller than those associated with the lifetime recovery reported for silicon hyperdoped with titanium[7,9,18] and consistent with the theoretical prediction of no lifetime recovery made in ref. 10. The contrast between these short lifetimes and the remarkable performance reported in ref. 3 for photodiodes made from these materials will be the subject of a future publication.

1) B. P. Bob, A. Kohno, S. Charnvanichborikarn, J. M. Warrender, I. Umezu, M. Tabbal, J. S. Williams, and M. J. Aziz: J. Appl. Phys. **107** (2010) 123506.
2) S. H. Pan, D. Recht, S. Charnvanichborikarn, J. S. Williams, and M. J. Aziz: Appl. Phys. Lett. **98** (2011) 121913.
3) A. J. Said, D. Recht, J. T. Sullivan, J. M. Warrender, T. Buonassisi, P. D. Persans, and M. J. Aziz: Appl. Phys. Lett. **99** (2011) 073503.
4) J. E. Carey, C. H. Crouch, M. Shen, and E. Mazur: Opt. Lett. **30** (2005) 1773.
5) M. U. Pralle and J. E. Carey: US-DOE Final Program Report SOI-0901-004 (2010).
6) I. Umezu, A. Kohno, J. M. Warrender, Y. Takatori, Y. Hirao, S. Nakagawa, A. Sugimura, S. Charnvanichborikarn, J. S. Williams, and M. J. Aziz: AIP Conf. Proc. **1399** (2011) 51.
7) M. T. Winkler, D. Recht, M. Sher, A. J. Said, E. Mazur, and M. J. Aziz: Phys. Rev. Lett. **106** (2011) 178701.
8) J. T. Sullivan, R. G. Wilks, M. T. Winkler, L. Weinhardt, D. Recht, A. J. Said, B. K. Newman, Y. Zhang, M. Blum, S. Krause, W. L. Yang, C. Heske, M. J. Aziz, M. Bär, and T. Buonassisi: Appl. Phys. Lett. **99** (2011) 142102.
9) E. Antolin, A. Marti, J. Olea, D. Pastor, G. González-Diaz, I. Mártil, and A. Luque: Appl. Phys. Lett. **94** (2009) 042115.
10) J. J. Krich, B. I. Halperin, and A. Aspuru-Guzik: arXiv:1110.5639.
11) S. Deb and B. R. Nag: J. Appl. Phys. **33** (1962) 1604.
12) J. D. Holm and K. S. Champlin: J. Appl. Phys. **39** (1968) 275.
13) J. Eikelboom, C. Leguijt, C. Frumau, and A. Burgers: Sol. Energy Mater. Sol. Cell **36** (1995) 169.
14) R. Ahrenkiel and S. Johnston: Sol. Energy Mater. Sol. Cell **92** (2008) 830.
15) J. Borrego, R. Gutmann, N. Jensen, and O. Paz: Solid-State Electron. **30** (1987) 195.
16) R. A. Sinton and A. Cuevas: Appl. Phys. Lett. **69** (1996) 2510.
17) M. N. Afsar and H. Chi: Int. J. Infrared Millimeter Waves **15** (1994) 1181.
18) E. Ertekin, M. T. Winkler, D. Recht, A. J. Said, M. J. Aziz, T. Buonassisi, and J. C. Grossman: Phys. Rev. Lett. **108** (2012) 026401.
19) J. G. Fossum, R. P. Mertens, D. S. Lee, and J. F. Nijs: Solid-State Electron. **26** (1983) 569.